Research Article | Vol. 25, No. 25 | 11 Dec 2017 | OPTICS EXPRESS 31948
Optics EXPRESS

Enhancement of the damage resistance of ultra-fast optics by novel design approaches

THOMAS WILLEMSEN,[1,2,*] MARCO JUPÉ, [2] MARK GYAMFI,[2] SEBASTIAN SCHLICHTING,[2] AND DETLEV RISTAU[1,2]

[1]*Institut für Quantenoptik Quest, Leibniz Universität Hannover, 30167 Hanover, Germany*
[2]*Laser Zentrum Hannover e.V., Hollerithallee 8, 30419 Hanover, Germany*
**t.willemsen@lzh.de*

Abstract: Dielectric components are essential for laser applications. Chirped mirrors are applied to compress the temporal pulse broadening crucial in the femtosecond regime. However, the design sensitivity and the electric field distribution of chirped mirrors is complex often resulting in low laser induced damage resistances. An approach is presented to increase the damage resistance of pulse compressing mirrors up to 190% in the NIR spectral range. Layers with critical high field intensity of a binary mirror design are substituted by ternary composites and quantized nanolaminates, respectively. The deposition process is improved by an in situ technique monitoring the phase of reflectance.

OCIS codes: (310.0310) Thin films; (310.6860) Thin films, optical properties; (310.1860) Deposition and fabrication; (310.4165) Multilayer design; (320.0320) Ultrafast optics; (320.1590) Chirping.

References and links

1. S. Rausch, T. Binhammer, A. Harth, J. Kim, R. Ell, F. X. Kärtner, and U. Morgner, "Controlled waveforms on the single-cycle scale from a femtosecond oscillator," Opt. Express **16**(13), 9739–9745 (2008).
2. R. Szipöcs, K. Ferencz, C. Spielmann, and F. Krausz, "Chirped multilayer coatings for broadband dispersion control in femtosecond lasers," Opt. Lett. **19**(3), 201–203 (1994).
3. V. Pervak, O. Razskazovskaya, I. B. Angelov, K. L. Vodopyanov, and M. Trubetskov, "Dispersive mirror technology for ultrafast lasers in the range 220–4500 nm," Adv. Opt. Technol. **3**(1), 55–63 (2014).
4. D. Ristau, H. Ehlers, T. Gross, and M. Lappschies, "Optical broadband monitoring of conventional and ion processes," Appl. Opt. **45**(7), 1495–1501 (2006).
5. T. Willemsen, S. Schlichting, M. Gyamfi, M. Jupé, H. Ehlers, U. Morgner, and D. Ristau, "Improved LIDT values for dielectric dispersive compensating mirrors applying ternary composites," Proc. SPIE **10014**, 100141Z (2016).
6. D. Ristau, *Laser-Induced Damage in Optical Materials* (CRC, 2014).
7. B. Mangote, L. Gallais, M. Commandré, M. Mende, L. Jensen, H. Ehlers, M. Jupé, D. Ristau, A. Melninkaitis, J. Mirauskas, V. Sirutkaitis, S. Kičas, T. Tolenis, and R. Drazdys, "Femtosecond laser damage resistance of oxide and mixture oxide optical coatings," Opt. Lett. **37**(9), 1478–1480 (2012).
8. M. Lappschies, B. Görtz, and D. Ristau, "Application of optical broadband monitoring to quasi-rugate filters by ion-beam sputtering," Appl. Opt. **45**(7), 1502–1506 (2006).
9. A. Melninkaitis, T. Tolenis, L. Mažulė, J. Mirauskas, V. Sirutkaitis, B. Mangote, X. Fu, M. Zerrad, L. Gallais, M. Commandré, S. Kičas, and R. Drazdys, "Characterization of zirconia- and niobia-silica mixture coatings produced by ion-beam sputtering," Appl. Opt. **50**(9), C188–C196 (2011).
10. M. Jupe, M. Lappschies, L. Jensen, K. Starke, and D. Ristau, "Improvement in laser irradiation resistance of fs-dielectric optics using silica mixtures," Proc. SPIE **6403**, 64031A (2007).
11. M. Jupé, M. Lappschies, L. Jensen, K. Starke, D. Ristau, A. Melninkaitis, and W. Rudolph, "Mixed oxide coatings for advanced fs-laser applications," Proc. SPIE **6720**, 67200U (2007).
12. H. Kroemer, "Heterostructure bipolar transistors and integrated circuits," in *Proceedings of the IEEE*, (IEEE, 1982), pp. 13–25.
13. T. Willemsen, M. Jupé, L. Gallais, D. Tetzlaff, and D. Ristau, "Tunable optical properties of amorphous Tantala layers in a quantizing structure," Opt. Lett. **42**(21), 4502–4505 (2017).
14. T. Willemsen, P. Geerke, M. Jupé, L. Gallais, and D. Ristau, "Electronic quantization in dielectric nanolaminates," Proc. SPIE **10014**, 100140C (2016).
15. S. Schlichting, T. Willemsen, H. Ehlers, U. Morgner, and D. Ristau, "Fourier-transform spectral interferometry for in situ group delay dispersion monitoring of thin film coating processes," Opt. Express **24**(20), 22516–22527 (2016).
16. ISO 21254, "Lasers and laser-related equipment – Test methods for laser-induced damage threshold," (2011).

#309532 https://doi.org/10.1364/OE.25.031948
Journal © 2017 Received 20 Oct 2017; revised 27 Nov 2017; accepted 6 Dec 2017; published 7 Dec 2017

Optics EXPRESS

17. S. Schlichting, K. Heinrich, H. Ehlers, and D. Ristau, "Online re-optimization as a powerful part of enhanced strategies in optical broadband monitoring," Proc. SPIE **8168**, 81681E (2011).
18. T. Willemsen, S. Schlichting, T. Kellermann, M. Jupé, H. Ehlers, U. Morgner, and D. Ristau, "Precise fabrication of ultra violet dielectric dispersion compensating mirrors," Proc. SPIE **9627**, 96271U (2015).
19. J. Tauc, R. Grigorovici, and A. Vancu, "Optical properties and electronic structure of amorphous germanium," Phys. Status Solidi **15**(2), 627–637 (1966).
20. M. Beaudoin, M. Meunier, and C. J. Arsenault, "Blueshift of the optical band gap: Implications for the quantum confinement effect in a-Si:H/a-SiNx:H multilayers," Phys. Rev. B Condens. Matter **47**(4), 2197–2202 (1993).
21. B. Tatian, "Fitting refractive-index data with the Sellmeier dispersion formula," Appl. Opt. **23**(24), 4477–4485 (1984).
22. M. Cevro, "Ion-beam sputtering of (ta2o5) x (sio2) composite thin films," Thin Solid Films **258**(1–2), 91–103 (1995).
23. C. Kittel, *Introduction to Solid State Physics* (John Wiley, 1966).
24. P. S. Zory, *Quantum Well Lasers* (Academic, 1993).
25. A. V. Tikhonravov and M. K. Trubetskov, "OptiLayer software," http://www.optilayer.com
26. V. Pervak, M. K. Trubetskov, and A. V. Tikhonravov, "Robust synthesis of dispersive mirrors," Opt. Express **19**(3), 2371–2380 (2011).
27. T. V. Amotchkina, M. K. Trubetskov, V. Pervak, S. Schlichting, H. Ehlers, D. Ristau, and A. V. Tikhonravov, "Comparison of algorithms used for optical characterization of multilayer optical coatings," Appl. Opt. **50**(20), 3389–3395 (2011).
28. F. X. Kärtner, N. Matuschek, T. Schibli, U. Keller, H. A. Haus, C. Heine, R. Morf, V. Scheuer, M. Tilsch, and T. Tschudi, "Design and fabrication of double-chirped mirrors," Opt. Lett. **22**(11), 831–833 (1997).

1. Introduction

The rapid development of ultra-fast laser applications imposes high demands on dielectric optics designed for the femtosecond regime. Especially, optical components in the ultra-short laser resonator are playing a key role for further improvements of the decoupled laser parameters with respect to the maximum power and the achievable temporal pulse width [1]. In this context, the control of the temporal width of the laser pulse requires a precise phase management to counter the natural dispersion of light. Dielectric optics, so called chirped mirrors, offer the possibility to control the electric field of the light [2]. Nowadays various chirped mirrors are commercially available covering a broad range from the visible to the near infra-red spectral range as well as the requested laser pulse parameters [3]. Ion-Beam-Sputtering (IBS) in combination with precise optical monitoring techniques is considered as one of the best concept for the deposition of high quality ultra-short pulse optics [4]. However, the spectral performance remains very sensitive towards small deviations in layer thickness, and therefore, the precise deposition of the designs is still a demanding challenge in optical coating technology. In addition, the electric field distribution is complex in chirped mirror designs, and layers with highest field intensities are often located deep inside the layer stack [5]. High electric field layers affect the laser induced damage threshold (LIDT) of the coating systems and have to be evaluated in respect to their material properties [6]. For example, the LIDT is decreased for dielectric amorphous high refractive index materials (lower optical gaps) compared to low refractive index materials characterized by higher optical gap values [7]. In general only a limited amount of binary oxide materials are available to meet the high spectral requirements for amorphous dielectric thin films. Further significant improvements to increase the LIDT of binary materials are not expected. In order to achieve further progresses, novel design techniques are required to substitute high field intensity layers by materials with adjustable optical gap values and indices of refraction. A state of the art deposition concept to tune these parameters originates from the Ion-Beam-Co-Sputtering of at least two binary oxide materials [8]. For instance, a zone target consisting of two adjacent materials can be moved in front of the ion beam source and different fractions of both materials can be simultaneously sputtered to form a ternary dielectric with a composition according to the area fractions of the material zones interacting with the ion beam. The optical gap can be adjusted in between the values of both binary materials depending on the target position. The LIDT is increased for higher optical gap values in correlation with a decreasing index of refraction [9, 10]. As a consequence, a new class of ternary composite materials is

Optics EXPRESS

made available to optimize the LIDT of high reflective mirrors applying refractive index step down concept (RISED) [11]. The second approach is based on the manipulation of the electron confinement by a direct quantization of the binary material. This principle is well known for crystalline semiconductor materials [12]. A material with a low optical gap (quantum well) is embedded in a matrix of a high optical gap material (barrier). The electronic structure of the materials is controlled by the thickness of the quantum well through the electron confinement in between the barriers. Layers of these nanostructures, called nanolaminates, allow the fabrication of materials with optical properties different to the host materials. In amorphous materials the microscopic long range order is missing with respect to crystalline materials, and a formation of a dielectric quantized layer stack is not obvious. However in recent studies the change of the electron confinement of dielectric materials was successfully demonstrated in elementary studies [13, 14].

In this contribution, the fabrication of nanolaminates and ternary oxides are investigated to increase the laser induced damage threshold of chirped mirrors by substituting critical layers affected by high field intensities with these novel materials. In a first step, single ternary composite layers are compared to equivalent nanolaminate stacks with respect to the evolution of the optical gap in contrast to the refractive index and laser induced damage thresholds. Afterwards, the second section is dedicated to a design synthesis to evaluate a chirped mirror design suitable to compress a laser pulse for the NIR spectral range. The electric field distribution is analyzed, and critical layers are substituted by various ternary composites or quantized layer stacks. The sensitive deposition process is significantly improved applying an enhanced monitoring technique, whereby the group delay dispersion (GDD) of the growing layer structure is monitored directly in situ on moving substrates [15]. Finally the novel design approaches for the chirped mirrors are qualified by LIDT measurements in the fs regime according to ISO 21254 [16].

2. Deposition process and characterization methods

An Ion-Beam-Co-Sputter process is employed to manufacture all presented samples. The ion beam is extracted from an Argon gas plasma by a three grid system (Veeco 6 cm) and is directed on a linear translation stage loaded with Tantalum and Silicon targets. If the target table is moved in respect to the ion beam, both, ternary composites and binary dielectric layers can be sputtered in a reactive oxygen atmosphere to achieve a balanced stoichiometry. A sufficient precision in film thickness is attained with a highly developed broadband optical monitoring system (BBM) [4]. Respective transmittance measurements are recorded after every finished layer within a spectral wavelength range from 420 to 1050 nm. Possible deposition errors in particular layers can be corrected online during the coating process applying a reoptimization tool, which synchronously evaluates the recorded transmittance data. Employing a refinement algorithm, the subsequent layers can be optimized with respect to e.g. the specified GDD and reflection target values. An optimization cycle can be performed in situ after every coated layer [17]. Nanolaminate sequences with film thicknesses smaller than 2 nm are sputtered applying well-calibrated temporal monitoring. In addition the sensitive last layers of the manufactured chirped mirrors are switched applying a fiber based white light interferometer in combination with a fast high resolution spectrometer. The current in situ group delay dispersion curve is measured every time the moving sample is passing the measurement channel. For a precise layer termination, the current in situ GDD measurement curve is continuously compared to the theoretic design GDD curve of the particular layer. The available wavelength range of the in situ phase monitor covers a wavelength range from 810 nm up to 870 nm under an angle of incidence (AOI) of 0° [15]. The monitoring concept can be extrapolated to chirped mirrors with target specification differing in the wavelength regime [6, 18]. After post production the samples are characterized ex-situ applying a home build white light interferometer operating in the frequency domain and covering a wavelength range from 775 nm till 875 nm. The optical

Optics EXPRESS

properties of the deposited samples were derived from transmittance and reflectance spectrophotometric measurements (PerkinElmer – Lambda1050). On the basis of the obtained absorption coefficient α(ω), a Tauc approximation is applied to determine the optical gap [19]. Intermedia states are influencing the analysis of the absolute optical gap values; however a relative comparison is attainable by the Tauc formalism [20]. The laser induced damage threshold is measured for all samples applying S:1 tests according to ISO 21254. All LIDT measurement performed in this study are evaluated after an irradiation of 10,000 pulses. The laser pulses parameters are defined by p-polarized light at a center wavelength of λ_c = 775 nm, a pulse duration of τ_P = 150 fs with a repetition rate of 1 kHz and an effective beam width of d_{Beam} = 115 µm. The respective samples are irradiated under an AOI of 0°. The measurement uncertainty for the retrieved LIDT values can be estimated with 10%, because of the uncertainty of fluence values used for the tests.

3. Qualification of the materials

Layers affected by high field intensities can be exchanged if the optical gap value and index of refraction of the new material class is well characterized. In total eight ternary composites $Ta_xSi_yO_z$ are manufactured applying the described Ion-Beam-Co-Sputter technique. The optical parameters are extracted for samples with a total thickness of 300 nm, and the corresponding spectral behavior allows the determination of the refractive indices with sufficient precision (± 1%) applying the Sellmeier formalism [21]. The optical gap value can be increased by ΔE_{gap} = 1.06 eV with respect to a single Ta_2O_5 layer with a determined optical gap of 4.29 eV [22]. As the Silica content is increased in the ternary composites layers, the index of refraction decreases to 1.47 within this interval (compare black data points in Fig. 1) simultaneously with increasing higher optical gap values. The optical gap of a pure Silica layer is measured to a value of (7.2 ± 0.1) eV.

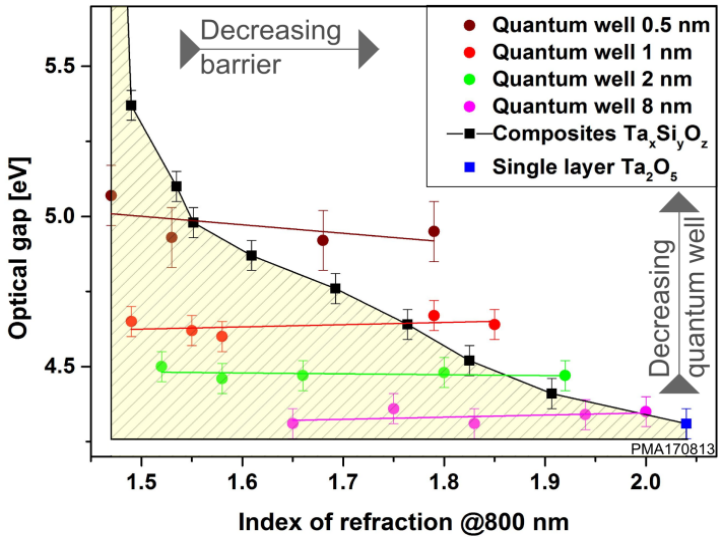

Fig. 1. Evolution of the optical gap plotted against the index of refraction for various ternary composites and nanolaminate sequences.

In contrast to ternary composites, the optical gap value of nanolaminates can be tuned by varying the thickness of the quantum well according to a finite potential well model based on the Schrödinger formalism. Depending on the applied materials, electrons can tunnel into barrier layers of a nanolaminate stack. The tunnel length can be approximated by an exponential decay [13, 23]. A maximum effective tunnel length into the SiO_2-barriers results to L_{eff} = 0.2 nm for Ta_2O_5 as quantum well. Consequently, the optical gap is expected to

Optics EXPRESS

remain constant for a fixed quantum well thickness while varying the barrier thickness above the calculated limit. In contrast, a variation of the index of refraction, which depends on relation of the content of the quantum well and barrier material, should be observed. Four series of nanolaminate stacks were manufactured to study this effect. For every chosen quantum well thickness of 8, 2, 1 or 0.5 nm (compare colored data points in Fig. 1) the barrier thicknesses are varied from 20 down to 10, 5, 1 and 0.5 nm. The periodic design structure is set to $(LH)^nL$. The respective number n of layer pairs is chosen to achieve a total design thickness of about 3 QWOT at λ_c = 800 nm, except for samples with a barrier thickness of 1 nm. These samples have the same total content of the high refractive index material as samples with barriers of 10 nm to prevent a blue shift caused by a lower Tantala content. The nanolaminate sequences can be treated as single dielectric layers with respect to their spectral behavior in transmittance and reflectance. The optical gap is analyzed in contrast to the refractive index at a wavelength of 800 nm and remains constant for a linearly increasing index of refraction. Nanolaminate stacks with quantum wells smaller or equal than 2 nm exhibit higher indices of refraction with respect to similar optical gap values of ternary composites. This result supports clearly the starting change of the electron confinement for quantum wells smaller than 4 nm depicted by a blue shift of the optical spectrum [13]. In summary, the linear increasing index of refraction for constant optical gaps signifies a major advantage of nanolaminates compared to ternary composites.

In a next step the manufactured ternary composites and nanolaminate samples are characterized with respect to the laser induced damage threshold. Both are compared by taking the relative LIDT H_{rel} into account:

$$H_{rel} = \frac{H \quad F_H}{H_{max} F_{H_{max}}}$$
$$\text{with} \quad F = \frac{n_{ref}}{n_0}|E|^2 \tag{1.1}$$

whereby H displays the retrieved LIDT values in J/cm^2, n_{ref} the index of refraction of the analyzed sample at a chosen center wavelength of λ_c = 800 nm, n_0 describes the index of refraction of the incident medium (air) and $|E|^2$ displays the maximum field intensity in the respective sample. H_{max} = 1.5 J/cm^2 is retrieved as the maximum LIDT value for both, the nanolaminate sample (E_{gap} = 4.95 eV) and ternary composite (E_{gap} = 5.10 eV) below the substrate damage threshold. A comparison depicts a higher LIDT for nanolaminate sequences compared to ternary composites with an equivalent optical gap (Fig. 2.). Considering crystalline nanolaminate structures, the spectral electron density dn/dW starts at level $W_n = W_{C1}$ in the conduction band [24]. The energy levels W_n of the electrons are distributed discretely in the valance and conduction band and are depending on the effective mass of the electrons and holes. The levels can be calculated applying numerical solutions of Schrödinger equation. The increased level might also occur in amorphous nanolaminate structures. In future studies the electron dynamics need to be correlated to damage models quantitatively. The validation of the empirical study is expected to gain new perceptions of the materials.

Optics EXPRESS

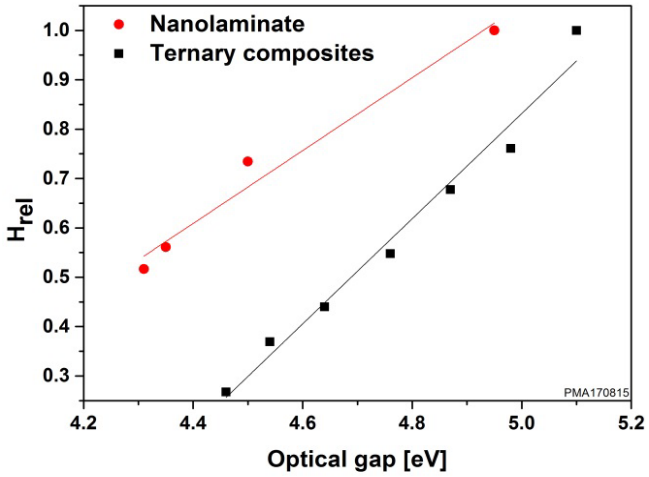

Fig. 2. Single ternary composites layers and nanolaminate stacks are compared with respect to the laser induced damage threshold. The respective retrieved LIDT values are determined with a maximum error of ± 10%. Afterwards the values are decoupled from the electric field and index of refraction and are normalized to their maximum value summarized as H_{rel}.

4. Design synthesis of chirped mirrors and resulting LIDT optimizations

The presented design studies were synthesized applying OptiLayer software [25]. The robust synthesis is applied to reduce the sensitivity of the design with respect to deposition errors during the manufacturing process. This synthesis uses a needle and gradual evolution algorithms for the design calculation [26, 27]. The distribution of the field intensity $|E|^2$ is analyzed by normalizing $|E|^2$ values to the field intensity of $|E|^2 = 100\%$. Since these values are quadratic, $|E|^2$ can reach 400% in the incident medium for the case of conventional QWOT high reflectors [25].

As design goals for the demonstrator, a group delay dispersion of –200 fs^2 and a reflectivity higher than 99.7% over the spectral range from 760 nm to 860 nm at an angle of incidence of 0° were chosen to represent a state of the art chirped mirror. A basic binary design consisting of Tantala and Silica layers was synthesized. This design consists of 82 layers, a total thickness of 8.1 µm and an average reflection value of 99.9% (Table 1), respectively. The distribution of the relative field intensity $|E|^2$ is analyzed, and Tantala layers with field intensity increased up to 390% occur deep inside the layer stack (Fig. 3 top). The binary Ta_2O_5 layer with maximum field intensity is deleted, and at this position a nanolaminate sequence or a ternary composite layer is inserted, respectively. In a first approach, this layer is replaced by a nanolaminate sequence with an optical gap value of 4.67 eV and a layer structure of $(LH)^5L$ (L = SiO_2 with a constant thickness of 20 nm per layer and H = Ta_2O_5 with a constant thickness of 1 nm per layer). A subsequent refinement is necessary to maintain the target specifications. The respective inserted nanolaminate structures and ternary composite layers are kept fixed during the refinement. In total this results in a 106 layer design with a total thickness of 8.9 µm and an average reflection of 99.9%. The maximum field intensity in a Ta_2O_5 layer is lowered by 190% with respect to the initial binary design. As a second alternative, the respective layer of the binary design is exchanged by a ternary $Ta_xSi_yO_z$ composite with a determined optical gap value of 4.76 eV. Four composite layers are implemented to reduce the field intensity in pure Ta_2O_5 layers down to 200% (Fig. 3).

Optics EXPRESS

Table 1. Design parameters of the manufactured chirped mirrors. For every design the target points are kept constant with respect to the wavelength range Δλ = 100 nm (from 770 to 870 nm) and the GDD of –200 fs².

Designs	Layers	Total thickness [µm]	Minimum reflection value[%]	Maximum $\|E\|^2$ in Ta_2O_5 layer [%]	Optical gap [eV] and maximum $\|E\|^2$ of substituted layers [%]
Initial binary design	82	8.1	99.9	390	—
CM applying ternary composites	68	7.9	99.6	175	4.76 $\|E\|^2_{max}$ = 280%
CM applying nanolaminate stacks	106	8.9	99.7	200	4.67 $\|E\|^2_{max}$ = 350%

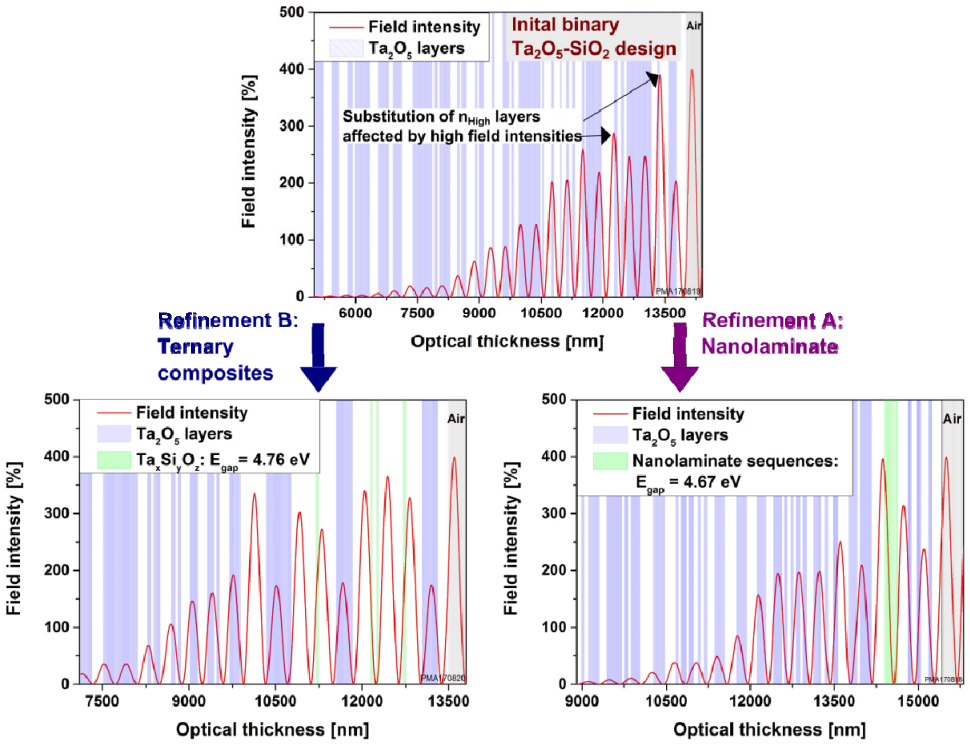

Fig. 3. Field intensities plotted against the optical design thicknesses. An initial binary Ta_2O_5-SiO_2 design is analyzed, and the Ta_2O_5 layers affected by a maximum in field intensities are substituted by nanolaminate sequences and ternary composites, respectively.

The measured group delay dispersion of the manufactured chirped mirrors is compared to the calculated design and data from reverse engineering algorithm based on the recorded in situ transmittance data. In addition the maximal deviation is plotted for estimated variations in layer thickness during the sputter process with respect to the target data (Fig. 4). A random distribution of a maximum change of the index of refraction of ± 1% and a maximum deposition error of the physical thickness of ± 1 nm for the last layers is estimated according to Optilayer procedure [25]. The plotted curve displays an average of 50 calculation runs of the maximal deviation. The measurement results are quantified taking into account the residual sum of squares

$$RSS = \sum_{i}^{n} (GDD_{dsg}(\lambda_i) - GDD_{rev}(\lambda_i))^2$$

Optics EXPRESS

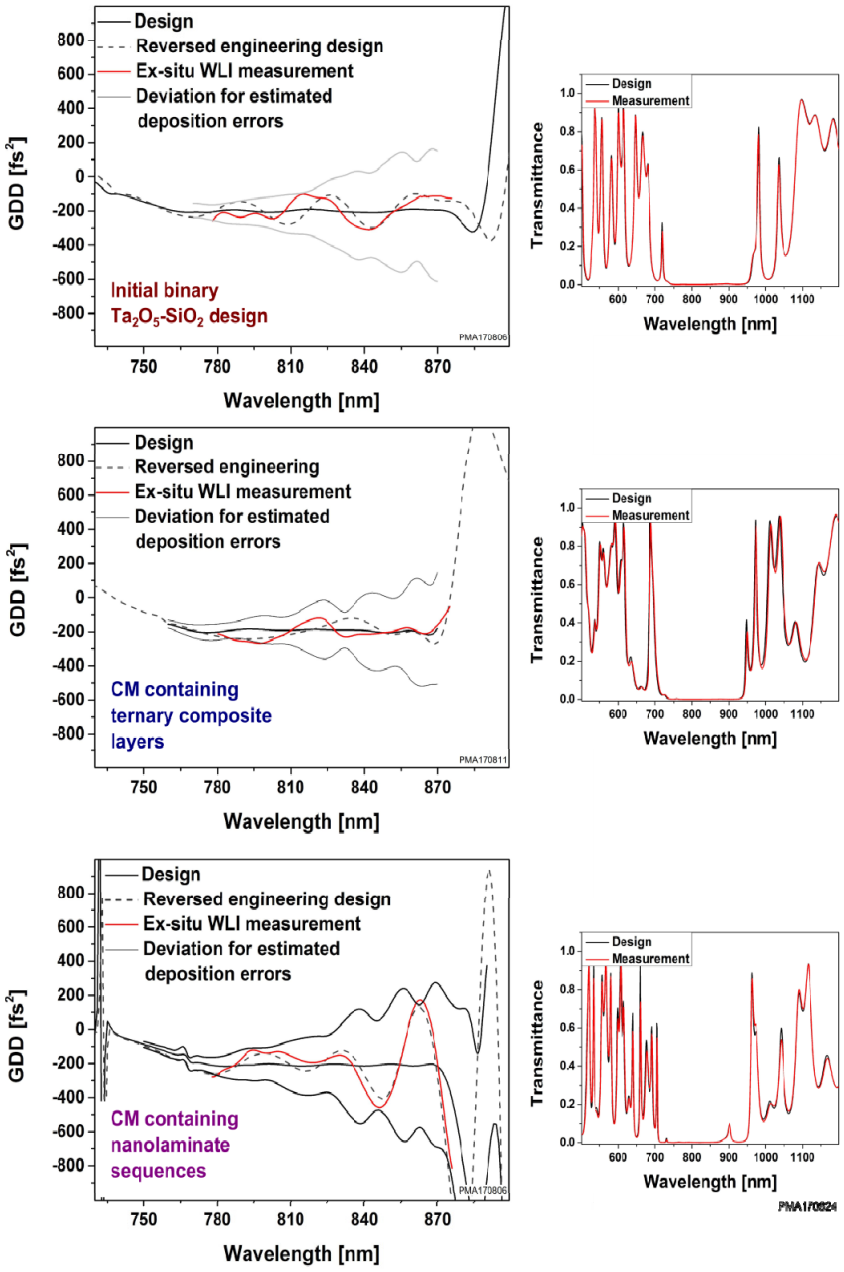

Fig. 4. Measured GDD spectra and transmittance scans for the manufactured chirped mirrors.

Whereby GDD_{dsg} is the initial calculated group delay dispersion design value and GDD_{rev} refers to the reversed engineering GDD, respectively. Both, the binary CM and the CM containing ternary composites deviate by a maximum of ± 100 fs^2 from the target value and have a similar RSS. However the mirror containing nanolaminate sequences reveals an increased RSS by a factor of 4, which is mainly caused by a major deviation between 840 and 860 nm with respect to the calculated design (Fig. 4 bottom). The design is shifted in central wavelength following the reversed engineering data. In between a spectral range from 750 to 840 nm a maximum GDD of ± 100 fs^2 can be observed resulting in a similar RSS with respect to the initial design. The respective transmittance scans are compared to the reversed

Optics EXPRESS

engineering designs and indicate no deviation from the set reflection target points (Fig. 4 respective right graphs). A significant change in the field intensity for the respective substituted layer structures and Ta_2O_5 layers with highest field intensity could not be observed analyzing the field intensities of the reversed engineering designs.

The LIDT measurements are evaluated after an irradiation with 10,000 pulses, and the respective values at a damage probability of 0% are assessed for comparing the three manufactured mirrors. The binary CM is characterized by an absolute LIDT value of (0.17 ± 0.02) J/cm^2. The substitution by ternary layers and nanolaminate sequences improve the LIDT by 170% and 188%, respectively (Fig. 6).

Three additional chirped mirrors were manufactured and characterized to verify the shown improvements in LIDT (Table 2).

Table 2. Design parameters of the manufactured chirped mirrors. For every design the target points are kept constant with respect to the wavelength range Δλ = 100 nm (from 770 to 870 nm) and the GDD of –200 fs^2.

Designs	Layers	Total thickness [µm]	Minimum Reflection value[%]	Maximum $\|E\|^2$ in Ta_2O_5 layer [%]	Optical gap [eV] and maximum $\|E\|^2$ of substituted layers [%]
E-Field optimized binary design	73	8.0	99.8	240	—
RISED CM applying ternary composites	74	7.3	99.4	175	5.1; 4.98; 4.87; 4.76; 4.64 $\|E\|^2_{max}$ = 250%
CM applying nanolaminate stacks	116	8.3	99.7	280	4.67; 4.97 $\|E\|^2_{max}$ = 490%

A binary chirped mirror was manufactured applying an electric field optimization target in the Optilayer software. The design is characterized by maximum field intensity in Ta_2O_5 layers of 240% and by a retrieved LIDT value of H = 0.22 J/cm^2. However, the design sensitivity is further increased and results in a maximum deviation of ± 170 fs^2 with respect to a GDD target value of –200 fs^2 (Fig. 5). Next, two CMs are manufactured and characterized applying several layer structures with varying optical gap values with respect to both, different ternary composites and different quantum wells of nanolaminate stacks. This design approach originates from the refractive index step down concept, which is successfully demonstrated for conventional high reflective mirrors [6]. Following this results, several layer structures with differing optical gaps are substituted in the initial binary design. First, three nanolaminate sequences are substituted in the initial binary design characterized by optical gaps of 4.95 eV ((HL)^{5}L, whereby H = 0.5 nm and L = 20 nm) and two sequences with E_{Gap} = 4.67 eV (((HL)^{4}L, whereby H = 1 nm and L = 20 nm) (Fig. 5 upper row), respectively. A maximum deviation of the GDD up to ± 400 fs^2 occurred following the reversed engineering data. The mirror can be applied for a pair of chirped mirrors (DCM) because of the systematic curve progression [28]. In a next step six differing ternary composites are substituted in the initial design. A range of the optical gap from 4.64 eV to 5.1 eV is covered, and the respective physical thicknesses are varied from 30 nm up to 122 nm.

Optics EXPRESS

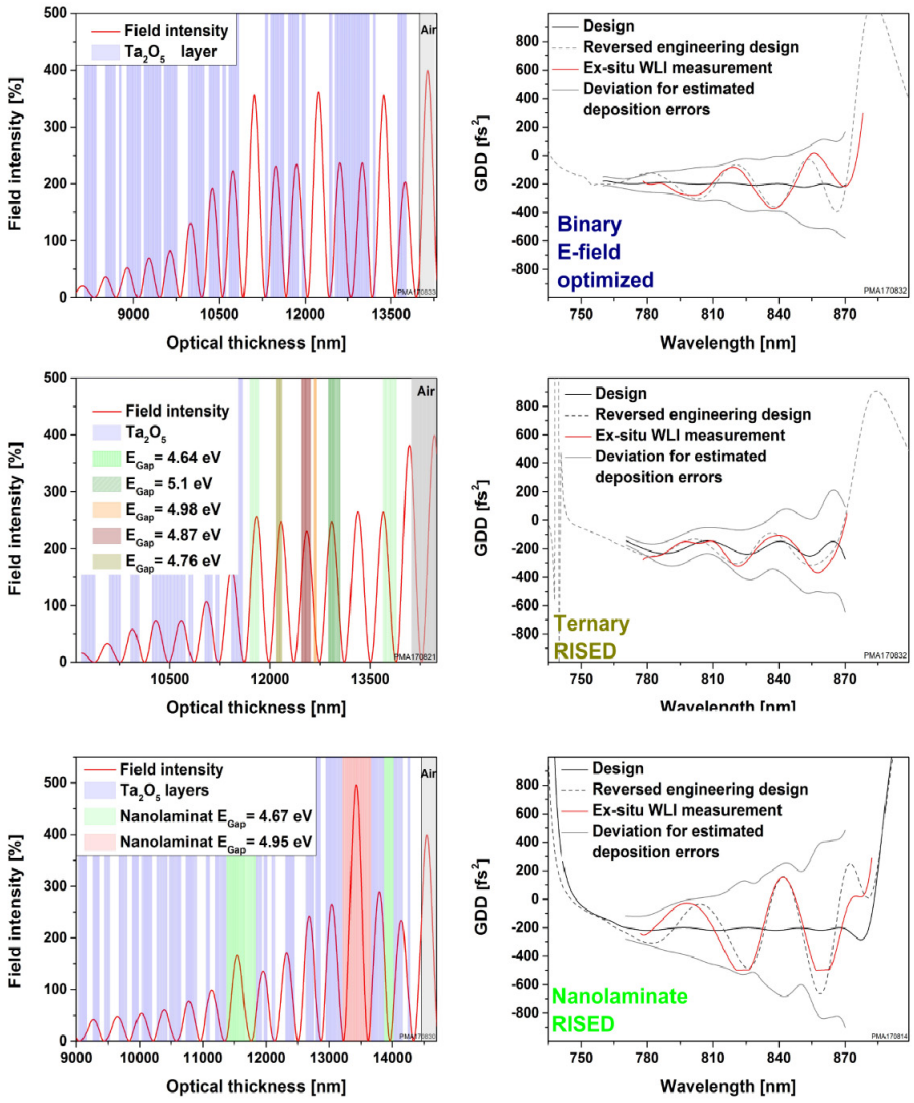

Fig. 5. Field intensities plotted against the optical design thicknesses and measured GDD spectra for the manufactured additional chirped mirrors.

The resulting LIDT values could not be further improved for the chirped mirror and are 50% higher than the binary design with an optimized E-field (Fig. 6).

In future studies, a slight change (<< 1%) of the index of refraction has to be evaluated for long time deposition coatings. This change impacts the relative error of the thin sputtered nanolaminate layers stronger than for thicker ternary composite layers. Nevertheless the caused deviation is still within the maximum calculated deviations (Compare grey solid lines in Fig. 4 and Fig. 5). A maximum deviation in layer thickness of ± 1 nm and a total change of the high index of refraction of ± 1% is estimated for the respective last 6 layers. Several deposition iterations of the design are expected to further minimize the sensitivity with respect to changing process parameters. As major advantages, nanolaminate sequences offer a higher LIDT value, and a complex zone target assembly is not required. In addition, the difference of the index of refraction can be kept high because of the tunable index of refraction for a constant optical gap.

Optics EXPRESS

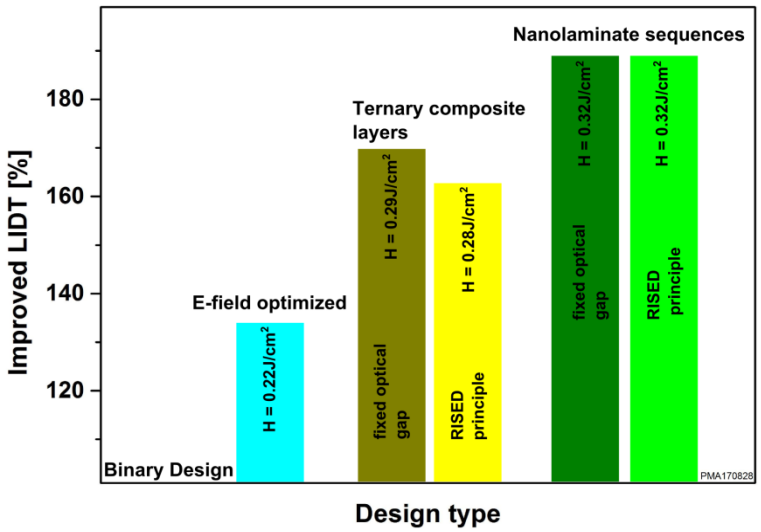

Fig. 6. Enhancement of the LIDT with respect to a binary oxide Ta_2O_5-SiO_2 chirped mirror. The initial binary design is represented by 100% and characterized by a LIDT of H = 0.17 J/cm^2.

A higher enhancement of the LIDT is expected by implementing nanolaminate sequences with lower quantum wells and lower barriers. This will impact both, a higher optical gap for an improved LIDT and a higher index of refraction to maintain the reflection target. The design concept of substituting high field intensity layers is expected to be independent of the applied binary materials. For instance, Hafnia has a significant higher laser induced damage threshold with respect to Tantala [7]. The application of HfO_2-SiO_2 nanolaminate sequences is expected to further increase the LIDT suitable to fulfil the next demands for high power optical components.

5. Conclusion

The presented study reports about the possibility to increase the laser induced damage threshold of complex dielectric optical components. The electric field distribution of high refractive index layers inside the layer stack is analyzed, and critical layers are substituted by stacks with improved optical gap values to enhance the laser induced damage threshold (LIDT). For this purpose two material classes are evaluated and compared. First the optical gap can be tuned by varying the oxide composition of two co-sputtered target materials. Second the electron confinement of the binary material itself can be changed in a quantizing structure. In correlation to the theoretical model, the index of refraction remains constant for a fixed quantum well with varying barriers. With respect to similar optical gap values of ternary composites, higher indices of refraction can be achieved for nanolaminate structures with quantum wells smaller than 4 nm. The weighted LIDT of nanolaminate structures is higher compared to equivalent ternary composites. Both, the tunable index of refraction and better LIDT performance are offering major advantages of nanolaminate structures. In a next step, a challenging design for compressing a femtosecond pulse is calculated applying binary oxide materials. Sensitive high field intensity layers are exchanged by appropriate ternary composites and quantized layer structures, respectively. The complex sputter process is improved by monitoring the group delay dispersion in reflectance on moving substrates. Final LIDT measurements of the manufactured and characterized chirped mirrors show an improved power handling capability up to 188% applying modified layer structures with respect to the binary mirror. The results are classified by comparing the LIDT values with an E-field optimized binary oxide design and by the application of several ternary composites

Optics EXPRESS

and nanolaminate structures with differing optical gaps. Future applications of modified nanolaminate structures with lower optical gaps and barriers are expected to further increase the LIDT. The concept is independent of the chosen binary materials and offers a high potential to cope with the increasing demands of optics necessary for the development of high power laser applications in the femtosecond regime.

Funding

Volkswagen Stiftung (Hymnos) (ZN3061); Deutsche Forschungsgemeinschaft (DFG) (Cluster of excellence 201 Quest).

Acknowledgments

The authors thank Malte Brinkmann for his contribution to this work.